

Investigation of annealing temperature on microstructure and texture of Fe-19Cr-2Mo-Nb-Ti ferritic stainless steel

Guojun Cai, Changsheng Li*, Dongge Wang, Yongkang Zhou

State Key Laboratory of Rolling and Automation, Northeastern University, Shenyang 110819, PR China

ARTICLE INFO

Keywords:

Ferritic stainless steel
Annealing temperature
Texture
Formability
Plastic strain ratio

ABSTRACT

The evolution of microstructure and texture of Fe-19Cr-2Mo-Nb-Ti ferritic stainless steel annealed at different temperatures was investigated using a combination of X-ray diffraction (XRD) and electron backscatter diffraction (EBSD). EBSD investigations confirm that the in-grain shear bands provide more recrystallization nucleation sites to γ -fiber recrystallization grains with high Taylor factor orientations during cold rolling requiring further annealing for a more homogenous equiaxed grain structure. As the annealing temperatures increase, the grains in center layer are oriented towards $\{110\}\parallel\text{ND}$, and the recrystallization grains at 1050 °C are dominated by the uniform and equiaxed γ -fiber grains favourable for the improvement of r -values, while the occurrence of $\{100\}\langle 011\rangle$ texture detrimental to r -values indicates that an exorbitant annealing temperature can reduce the intensity of γ -fiber textures affecting the formability, accordingly, the average plastic strain ratio of ferritic stainless steel increases sharply up to a maximum value (1.69) and then decreases to a certain value (1.42).

1. Introduction

Recently, to replace AISI 304 austenitic stainless steels (ASSs) in most environments, a new type of heat resistant ferritic stainless steels (FSSs) with Nb, Ti and Mo alloying has been developed to be used in auto vent pipe which requires excellent corrosion-resistance and formability [1]. To obtain strong corrosion-resistance, the high Cr addition improves the corrosion resistance of stainless steel by the reinforcement of passive film, while the relatively high Ti and Nb additions lead to a less stable microstructure susceptible to some intermetallic compounds and carbonitrides, such as (Nb, Ti) (C, N) precipitates and Laves phases [2–4], known to noticeably influence high temperature oxidation resistance and thermal fatigue life. However, Fe-19Cr-2Mo-Nb-Ti ferritic stainless steel faces the challenge of the lower formability in contrast to ASSs, which restricts its manufacture and application in more fields.

In general, the formability of FSSs can be improved by r -values strongly relating with the texture evolution during annealing, which mainly depends on particular characteristics of γ -fiber ($\langle 111\rangle\parallel\text{ND}$) recrystallization texture, such as the orientation uniformity and intensity [5]. For this reason, Ray et al. [6] investigated that the formability of steel could be improved by increasing the r -values associated with the $\{111\}$ recrystallization texture. Huh and Engler [7] proposed that the more desirable γ -fiber recrystallization texture during intermediate annealing could cause a marked increase in the r -values. Shu et al. [8] pointed out that the Ti and Nb additions in 15%Cr ferritic stainless steel

obtained higher r -values and lower Δr values which were attributed to the high intensity and uniform γ -fiber texture comprising the $\{111\}\langle 112\rangle$ and $\{111\}\langle 110\rangle$ components. Yan et al. [9] suggested that the uniform and sharp γ -fiber recrystallization texture beneficial to the high r -values was attributable to the uniformity of grain size distribution and the fraction of coincidence site lattice.

The different annealing temperatures will have an influence on the precipitates, texture evolution and grain size distribution as a result of the recrystallization and grain growth phenomena. It is well known that the formability of ferritic stainless steels is function of its chemical composition, microstructure and texture, and the sequence of secondary phase nucleation in ferritic stainless steels can affect the texture evolution and applications at high service temperature. The aim in this study, the careful and overall work is to explain different annealing temperatures and obtain further knowledge about formability of Fe-19Cr-2Mo-Nb-Ti ferritic stainless steel improved by the precipitate behavior and texture evolution.

2. Materials and Methods

In this investigation, Fe-19Cr-2Mo-Nb-Ti ferritic stainless steel was made in a 150 kg high frequency vacuum induction furnace, whose chemical compositions were presented in Table 1.

After the ingot was forged into 50 mm sheet at 1050–850 °C, it was hot rolled to 3 mm thickness sheet by seven passes from 1150 °C to

* Corresponding author.

E-mail address: lics@ral.neu.edu.cn (C. Li).

<https://doi.org/10.1016/j.matchar.2018.04.031>

Received 30 September 2017; Received in revised form 13 April 2018; Accepted 20 April 2018

Available online 22 April 2018

1044-5803/ © 2018 Elsevier Inc. All rights reserved.

Table 1
Compositions of experimental steel (wt%).

C	Si	Mn	P	S	Cr	Nb	Ti	N	Mo	Fe
0.009	0.52	0.32	0.008	0.008	19.5	0.45	0.155	0.072	1.97	Bal.

850 °C on a Φ 450 mm hot rolling mill, and annealed at 1050 °C for 8 min in a Nitrogen atmosphere, then it was cold rolled to 1 mm in thickness by five passes. The conditions of the final annealing were 950 °C for 3 min, 1000 °C for 3 min, 1050 °C for 3 min, 1100 °C for 3 min, and then cooling in air.

The microstructures of samples with different annealing temperatures were obtained by etching in a solution of 4 g CuSO₄ + 30 mL HCl + 25 mL H₂O after preparing in a standard way. The element distribution of precipitates was investigated in Electron probe micro-analysis (EPMA), determined at an operating voltage of 20 kV and a current of 1.05×10^{-8} A. In order to further verify the evolution of textures, the microstructures along the longitudinal section as defined by the rolling direction (RD) and normal direction (ND) were studied using an FEI Quanta 600 scanning electron microscope (SEM) equipped with an OIM 4000 electron backscatter diffraction (EBSD) detector, and the orientation distribution functions (ODFs) had been measured and calculated in the center layer based on X-ray diffraction (XRD). The average *r*-values were measured using SANS CMT7000 universal testing machine, and machined at angles of 0° (*r*₀), 45° (*r*₄₅) and 90° (*r*₉₀) to the rolling direction (RD) for tensile tests.

3. Results

3.1. Microstructure and Precipitate

Fig. 1 reveals the crystallographic characteristics and frequency distribution of misorientation of hot-rolled sheet and annealed sheet analyzed by EBSD. As the figures show, red and black lines denote low-angle grain boundaries (LAGBs) with having the misorientation < 15°

and high-angle grain boundaries (HAGBs) having the misorientation > 15°, respectively. According to the frequency distribution of misorientation, the volume fraction of LAGBs within ferrite grains of annealed sheet is significantly decreased compared with the hot-rolled specimen, and elongated grains display a low ratio of HAGBs (Fig.1b) while almost equiaxed grains exhibit a high ratio of HAGBs (Fig.1d).

Fig. 2 displays the microstructures of sheets with different annealing temperatures. The average grain size of sheets has been measured by the linear intersect method and the results indicate that the average grain size increases with the increase of annealing temperature. After annealing at 950 °C, the fine and homogeneous precipitates can influence the grain size (10–30 μm) because of their pinning effect in contrast to large-sized precipitates existing in 1100 °C annealed sheet.

In order to clearly demonstrate the microstructure and composition of precipitates, Fig. 3 reveals the EPMA elemental mapping analysis of precipitates in 950 °C annealed sheet. It is evident that there are two types of precipitates: the (Nb, Ti) (C, N) precipitate and (Fe, Cr)₂ (Nb,Ti) type Laves phase, examined and classified by EPMA elemental mapping analysis and the analysis of energy spectrum, and the mass concentration (%) of each element is identified by various degrees of contrast and colors. The precipitates in 950 °C annealed sheet can be clearly distinguished from the distribution of Nb, Ti, C and N, and the size of (Nb,Ti)(C, N) precipitate is 286 nm, as well as a higher content of Nb and Ti in central area, and the size of long strip Laves phase containing Nb and Ti in 950 °C annealed sheet is approximately 625 nm.

3.2. Texture Evolution

Fig. 4 presents the orientation image map and corresponding $\varphi_2 = 45^\circ$ section of ODF of hot-rolled sheet and annealed sheet. There are some elongated grains with continuous {100} orientation comprising the cube orientation {100}<001> and rotating cube orientation {100}<011> in the center area, and a little indistinctive deformed grains with the {111} orientation as well as some Goss-oriented grains on the surface layer (Fig. 4a). Owing to the shear stress, Goss-oriented grains are nucleated mainly within or around the deformed elongate grains

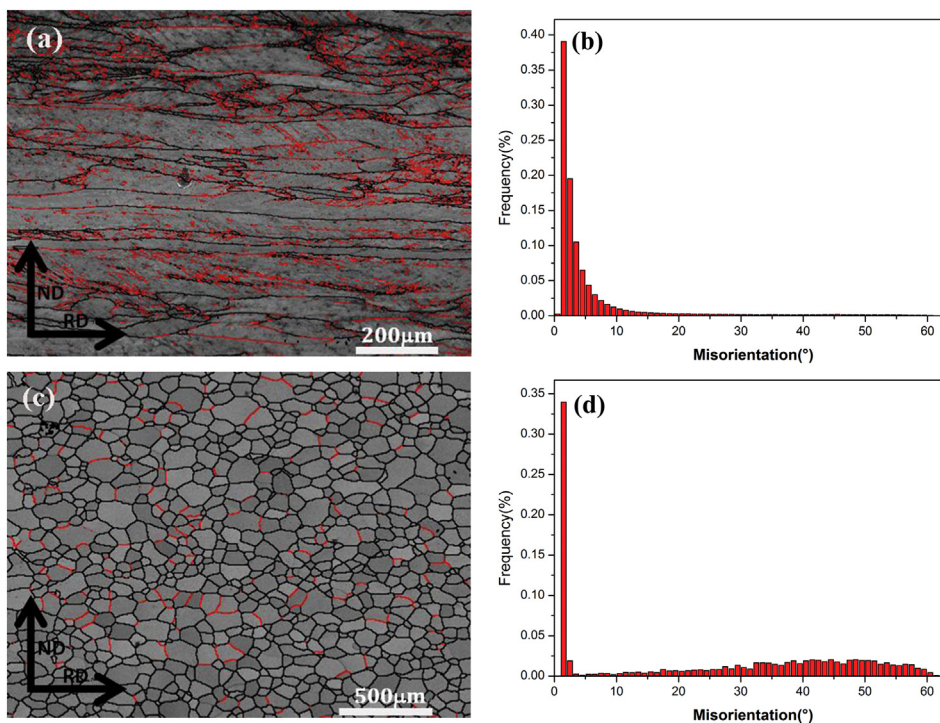


Fig. 1. Crystallographic characteristics (a, c) and frequency distribution of misorientation (b, d) of samples analyzed by EBSD: (a-b) hot-rolled sheet and (c-d) annealed sheet.

Download English Version:

<https://daneshyari.com/en/article/7969110>

Download Persian Version:

<https://daneshyari.com/article/7969110>

[Daneshyari.com](https://daneshyari.com)